Vol 18 No 10, October 2009
1674-1056/2009/18(10)/4418–07

Chinese Physics B

© 2009 Chin. Phys. Soc.
and IOP Publishing Ltd

# Lattice strain and *p-d* repulsion affecting electronic structure of wurtzite $Zn_{1-x}Cd_xO$ alloys

Shi Li-Bin(史力斌)†, Kang Li(康 莉), Jin Jian-Wei(金健维), and Chi Feng(迟 锋)

*Department of Physics, Bohai University, Jinzhou* 121013, *China*

(Received 20 January 2009; revised manuscript received 22 June 2009)

In the paper, density of states, band structure and electron density difference of $Zn_{1-x}Cd_xO$ are calculated by first principles, here $x$ varies from 0 to 0.75 at intervals of 0.125, and the band gap obtained from band structure changes from 0.968 eV to 0.043 eV. The lattice strain and *p-d* repulsion theory are used to investigate variation of the band gap, the results obtained show that the variation is mainly due to the lattice tensile strain. The *p-d* repulsion in $Zn_{1-x}Cd_xO$ cannot be neglected. In addition, electron density difference can be used to verify the results.

**Keywords:** first principles calculation, density of states, band structure, *p-d* repulsion
**PACC:** 7000, 7115M, 7125

## 1. Introduction

ZnO is an interesting solid with four different kinds of crystal structures, wurtzite, blende, rocksalt and CsCl.[1] Under an ambient condition, wurtzite takes on a stable structure. Due to its unique electronic, optical and piezoelectric properties, ZnO is regarded as an ideal material for making field effect transistors, light-emitting diodes, resonators, biosensors and piezoelectric devices.[2−4] ZnO generally exhibits n-type conduction because of the existence of oxygen vacancy and zinc interstitial in addition to pure ZnO. The fabrication of p-ZnO has proved to be difficult, which impedes practical application of the ZnO-based devices. Recently, Vaithianathan *et al*[5] and Kang *et al*[6] suggested that As-doped p-type ZnO can be obtained by replacing the O sites, forming $As_O$ and replacing the Zn sites, forming $As_{Zn}$. Xiao *et al*[7] found p-type conductivity in nitrogen-doped ZnO thin film.

Another problem in applications of ZnO is to tune the size of the band gap. One of the ways of doing this is to alloy ZnO with materials such as MgO and CdO. Due to the different crystalline structures of the binary compounds of MgO, CdO and ZnO, phase separation has been detected in the $Zn_{1-x}Mg_xO$, $Zn_{1-x}Cd_xO$ films,[8] which affects the quality of ZnO-based films. In addition, the residual stress is always inevitable in the ZnO films due to lattice mismatch between the substrate and the film. The strain or stress in ZnO can result in energy rise, and thus solubility fall of Mg and Cd in ZnO. Epitaxial growth can overcome the natural solubility limit of Mg and Cd, and tune the absorption edge from 2.1 eV to 4.4 eV.[9] At present, $Zn_{1-x}Cd_xO$ alloys with Cd concentration higher than 60% have been achieved, which is in accord with theoretical prediction.[10,11]

To understand the behavior of $Zn_{1-x}Cd_xO$, it is imperative to study both its crystal and electronic structures. Previously, there were a few reports on investigation of the electronic structure of $Zn_{1-x}Cd_xO$, where Cd concentrations are smaller than 25%.[12] In this paper, the electronic structure of the $Zn_{1-x}Cd_xO$ with $x$ ranging from 0 to 0.75 is investigated by first-principles. In addition, the strain and *p-d* repulsion are used to analyze the variation of band gaps.

## 2. Computational method

In this paper, all the calculations are performed using the CASTEP (Cambridge Serial Total Energy Package) code, which is based on density function theory and plane-wave pseudopotential method.[13,14] The exchange–correlation function is adopted in the generalized gradient approximation (GGA).[15] The interaction between valence electron and ion core is described by ultrasoft pseudopotential. Wurtzite $Zn_{1-x}Cd_xO$ with high Cd content can also be produced by epitaxial growth,[10] though the stable structure of $Zn_{1-x}Cd_xO$ will change from wurtzite to rocksalt with increasing Cd content. Therefore, the calculation is performed in the 2×2×1 wurtzite ZnO super-

†Corresponding author. E-mail: slb0813@sohu.com

cell. $Zn_{1-x}Cd_xO$ can be obtained by replacing the Zn on the sites with Cd, here $x$ changes from 0 to 0.75 at intervals of 0.125. The convergence tests of the total energy with respect to the plane wave cut-off energy and k-points sampling have been carefully examined (see Table 1). The final set of cut-off energy is 380 eV for the $Zn_{1-x}Cd_xO$ and the integration is performed using 4×4×5 k-point sampling which is generated by the Monkhorst–Pack scheme.

First, we optimize the crystal structures of the $Zn_{1-x}Cd_xO$ and then calculate their density of states and band structures. The optimization will finish if the convergence criterion is satisfied. (Maximum force between atoms is 0.03 eV/Å (1 Å=0.1 nm). Maximum stress is 0.05 GPa. Maximum displacement is $10^{-3}$ Å. Maximum energy change is $10^{-5}$ eV/atom.)

# 3. Results and discussion

## 3.1. The crystal structure

Table 1 shows optimized crystal parameters at different cut-off energies. The total energy hardly changes for ZnO/CdO when cut-off energy $E_{\rm cut}$ = 380 eV. The lattice constants $a$ = 3.258 Å/3.664 Å and $c$ = 5.262 Å/5.842 Å are in good agreement with the experimental and calculated values reported in Refs.[16] and [17], indicating that the calculation method used in this paper is rational. Because the ion radius of $Zn^{2+}$ is smaller than that of $Cd^{2+}$, the lattice constants of ZnO are a little smaller than those of CdO. The ratio ($c/a$) of ZnO is a little bigger than that of CdO. This difference of the ratios may come from different polarizations in ZnO and CdO.

**Table 1.** Geometry optimization of ZnO/CdO at different cut-off energies. $E_{\rm tot}$ and $V$ are energy and volume per cell, respectively.

| $E_{\rm cut}$/eV | $a$/Å | $c$/Å | $c/a$ | $E_{\rm tot}$/eV | $V$/Å$^3$ |
|---|---|---|---|---|---|
| 300 | 3.292/3.683 | 5.306/5.875 | 1.612/1.595 | –4310.937/–3450.531 | 49.811/69.026 |
| 320 | 3.280/3.676 | 5.284/5.864 | 1.611/1.595 | –4311.365/–3450.804 | 49.237/68.622 |
| 340 | 3.274/3.680 | 5.258/5.821 | 1.606/1.582 | –4311.535/–3450.929 | 48.805/68.277 |
| 360 | 3.268/3.668 | 5.257/5.846 | 1.607/1.594 | –4311.609/–3450.988 | 48.630/68.103 |
| 380 | 3.258/3.664 | 5.262/5.842 | 1.615/1.594 | –4311.627/–3451.009 | 48.398/67.937 |
| 400 | 3.258/3.664 | 5.256/5.840 | 1.613/1.594 | –4311.632/–3451.018 | 48.323/67.895 |
| Exp[16] | 3.253/- - - - | 5.213/- - - - | 1.603/- - - - | - - - -/- - - - | - - - -/- - - - |
| Cal[17] | 3.283/3.678 | 5.309/5.825 | 1.617/1.584 | - - - -/- - - - | - - - -/- - - - |

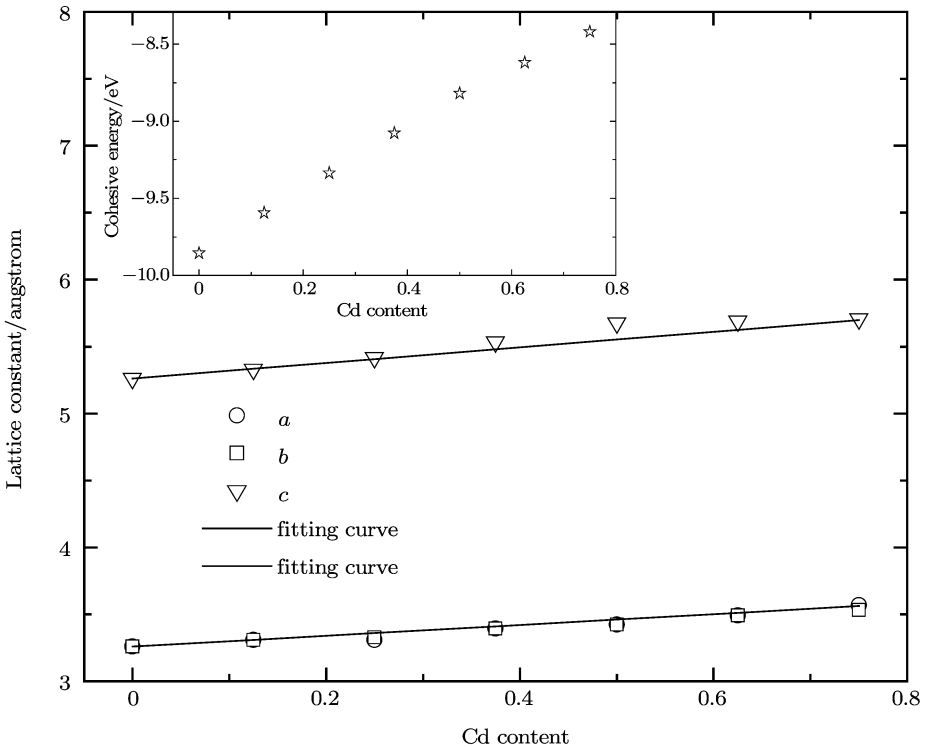



**Fig.1.** Lattice constants versus Cd content for $Zn_{1-x}Cd_xO$. Inset is the cohesive energy curve of $Zn_{1-x}Cd_xO$.

For $Zn_{1-x}Cd_xO$, the lattice constants increase with Cd content (see Fig.1). The lattice constants versus Cd content can be fitted by Vegard equation,[18]

$$a(x) = a_{CdO}x + a_{ZnO}(1-x), \quad (1)$$

$$c(x) = c_{CdO}x + c_{ZnO}(1-x), \quad (2)$$

where $x$ is the fraction of Cd in $Zn_{1-x}Cd_xO$. As seen from the inset of Fig.1, the cohesive energy of $Zn_{1-x}Cd_xO$ will increase with increasing Cd content, indicating that the structure stability of $Zn_{1-x}Cd_xO$ will fall.

## 3.2. Partial density of states

Figures 2 and 3 show partial density of states (PDOS) for ZnO and $Zn_{0.5}Cd_{0.5}O$, respectively, in which the top of the valence band is defined as 0 eV. For ZnO, the density of states in valence band mainly consists of the 2$s$, 2$p$ states of O and 3$d$ states of Zn. The density of states in the range from –6.0 eV to 0 eV is regarded as the upper valence band, which mainly comes from Zn 3$d$ and O 2$p$. The density of states near –17 eV is regarded as the lower valence band, which comes from O 2$s$. These results are consistent with previous calculation.[19] As seen from Fig.3, the upper valence band shows stronger non-local characteristics, which is in the range from –7.4 eV to 0 eV. The density of states of $d$ wave in the range from –7.4 eV to –6.0 eV mainly comes from 4$d$ of Cd. The energy level of Cd 4$d$ is lower than Zn 3$d$. The 2$p$ states of O hybridize with $d$ states of Zn and Cd in the range from –7.4 eV to –4.2 eV.

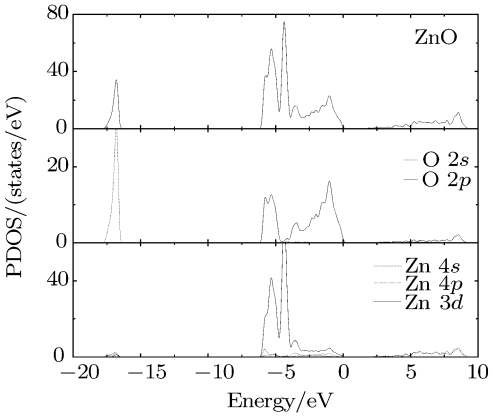



**Fig.2.** Partial density of states for ZnO.

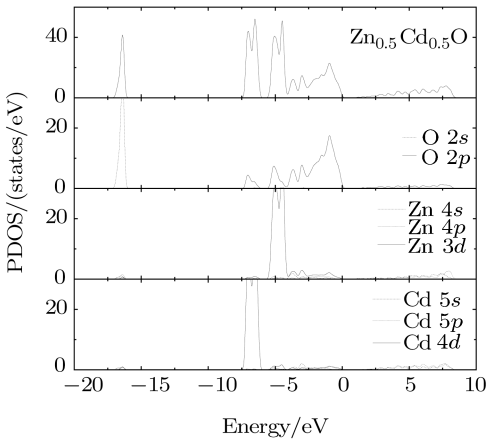



**Fig.3.** Partial density of states for $Zn_{0.5}Cd_{0.5}O$.

## 3.3. Band structure

Figures 4 and 5 show the band structures of ZnO and $Zn_{0.5}Cd_{0.5}O$, respectively. We can find that the bottom of conduction band and the top of valence band all appear at $\Gamma$ site, which indicates that $Zn_{1-x}Cd_xO$ is semiconductor with direct band gap. The values of band gap for ZnO and $Zn_{0.5}Cd_{0.5}O$ are 0.968 eV and 0.188 eV, respectively. The calculated value of band gap for ZnO is smaller than the experimental one 3.360 eV reported in Ref.[20]. It is well known that the exchange–correlation function in the GGA is underestimated, which is the cause of suppression for band gaps. As seen from Fig.4, the top of upper valence band is flat as compared with the bottom of conduction band near $\Gamma$ site, indicating that the cavity has a larger effective mass than the electron. This is a possible reason why it is difficult to obtain $p$-type ZnO by doping.[5–7]

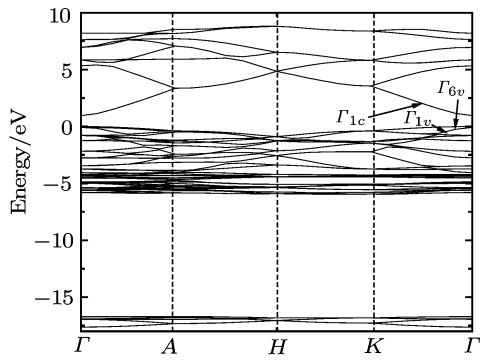



**Fig.4.** The calculated band structures for ZnO.

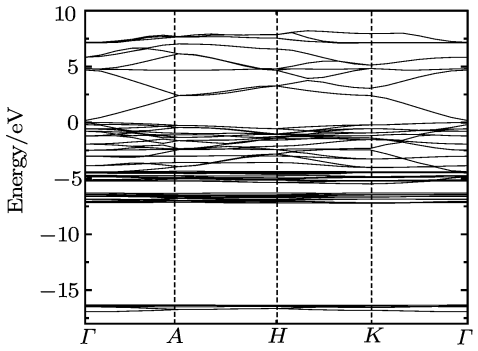



**Fig.5.** The calculated band structures for $Zn_{0.5}Cd_{0.5}O$.

The band gap of $Zn_{1-x}Cd_xO$ decreases with increasing Cd content and the values of which are shown in Table 2. The band gap of $Zn_{1-x}Cd_xO$ decreases to 0.043 eV as Cd content rises up to 0.75. In previous experiment, Ma *et al*[21] found that the band gap of $Zn_{1-x}Cd_xO$ can be modulated in the range from 3.3 eV to 2.65 eV as the Cd content changes from $x = 0$ to 0.5. The change of band gap is 0.65 eV, which is a little smaller than our result 0.78 eV (see Table 2). Therefore, the variation of band gap obtained from the first principles can be regarded as rational. Due to the lattice mismatch between CdO and ZnO, there is lattice strain in $Zn_{1-x}Cd_xO$, defined as $\varepsilon=(C - C_0)/C_0\times100\%$,[22] where $C$ is lattice constants ($a$, $b$, $c$) of strained ZnO, $C_0$ is lattice constants ($a = b = 3.258$ Å, $c = 5.262$ Å) of unstrained ZnO. The calculation is carried out in $a/b$-axis strain (the lattice constants in $a$-axis and $b$-axis change synchronously), and $c$-axis strain is found to change in the range from –0.2 to 0.2 at intervals of 0.05. The calculation also shows that ZnO is still a semiconductor with direct band gap when the strain in it changes. In Fig.6 are shown the values of band gap, in which the band gaps calculated from $c$-axis strain vary linearly with the strain. For $a/b$-axis strain, the variation of the band gaps shows as abnormal. Firstly, the band gaps increase linearly with $a/b$-axis strain changing from 0.2 to –0.05, and then fall exponentially. The curve of band gap versus strain can be fitted by a polynomial or exponential function, which is given in the caption of Fig.6. Usually, strain can result in variation of hybridization of atomic orbits, and the abnormal change of band gaps reflects the complexity of hybridisation and anisotropy of electron clouds distributed in space.

$E'_g$ in Table 2 denotes variation of band gap for $Zn_{1-x}Cd_xO$ due to lattice strains. Because the ionic radius of $Zn^{2+}$ is smaller than that of $Cd^{2+}$, Cd-doped ZnO will show tensile strain in $a/b$-axis and $c$-axis. As seen from Fig.6, the tensile strain in ZnO will result in the decrease of band gap, and from Table 2, the variation of band gap of $Zn_{1-x}Cd_xO$ is caused mainly by lattice tensile strain. The values of $\dfrac{(E'_g - E_0)}{(E_g - E_0)}$ will reduce when Cd content increases (here $E_0 = 0.968$ eV, corresponding to the band gap of unstrained ZnO). Strain may offer an opportunity to enhance the physical properties of materials. In a previous experiment, Li *et al*[23] pointed out that band gap of ZnO can be tuned by strain, and Liu *et al*[22] found that the strain in $Zn_{0.95}Co_{0.05}O$ films can enhance ferromagnetism, while our results show that the band gap of ZnO can be tuned by lattice strain.

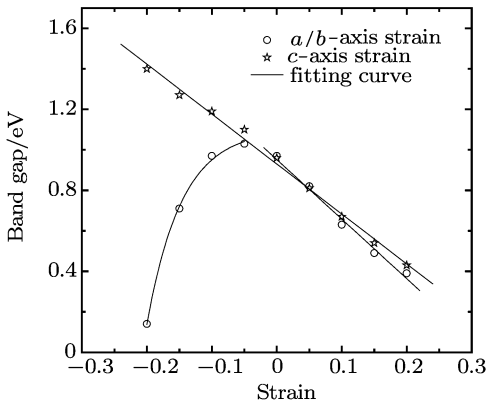



**Fig.6.** The band gap calculated from band structure versus strain for ZnO. For $a/b$-axis strain, the fitting equations are $E_g = -0.023\exp(-\varepsilon/0.054) + 1.100$ ($\varepsilon_{a/b} < -0.05$) and $E_g = 0.952 - 2.940\varepsilon$ ($\varepsilon_{a/b} > 0$), respectively. For $c$-axis strain, the fitting equation is $E_g = 0.932 - 2.467\varepsilon$.

**Table 2.** The variation of band gap of $Zn_{1-x}Cd_xO$ for different Cd contents. $E_g$ is the band gap for different Cd content. $E'_g$ is the band gap at different lattice strains which come from replacing Zn by Cd. $E_0 = 0.968$ eV.

| | Cd content | | | | | | |
|---|---|---|---|---|---|---|---|
| | 0.000 | 0.125 | 0.250 | 0.375 | 0.500 | 0.625 | 0.750 |
| $E_g$/eV | 0.968 | 0.732 | 0.511 | 0.341 | 0.188 | 0.122 | 0.043 |
| $E'_g$/eV | 0.968 | 0.783 | 0.624 | 0.528 | 0.443 | 0.408 | 0.360 |
| $\dfrac{E'_g - E_0}{E_g - E_0}$ | ... | 0.785 | 0.753 | 0.701 | 0.673 | 0.662 | 0.657 |

$Zn_{1-x}Cd_xO$ has a local tetrahedral environment, where Zn or Cd is surrounded by four O ions. According to *p-d* hybridisation theory, the band-state representations of $B_4$ at the Brillouin-zone center can be written as,[24]

$$\Gamma_{1c} \rightarrow s \text{ states} + f \text{ states} + g \text{ states}, \tag{3}$$

$$\Gamma_{6v} \rightarrow p(p_x, p_y, p_z) \text{ states} + d(d_{xy}, d_{yz}, d_{zx}) \text{ states} + f \text{ states}, \tag{4}$$

$$\Gamma_{1v} \rightarrow p(p_x, p_y, p_z) \text{ states} + d(d_{xy}, d_{yz}, d_{zx}) \text{ states} + f \text{ states}. \tag{5}$$

The *p-d* hybridisation makes an upward shift of $\Gamma_{6v}$ relative to the case without *p-d* hybridisation, which indicates that *p-d* states have repulsion. For binary compounds, the *p-d* repulsion energy ($\Delta E_{pd}$) is in proportion to the width of upper valence band, and in inverse proportion to the energy difference between anion-*p* orbit and cation-*d* orbit. In order to analyse variation of the band gaps, we calculate the *p-d* repulsion energy, the coupling matrix element of *p-d* orbit ($V_{pd}$) and the percent of *d* states in the antibonding state ($q$) by the equations[25]

$$\frac{1}{1-q} = 1 + \left(\frac{\Delta E_{pd}}{V_{pd}}\right)^2, \tag{6}$$

$$(E_p - E_d)^2 = \Delta E^2 - 4V_{pd}^2, \tag{7}$$

$$\Delta E = c(E_p - E_d + 2\Delta E_{pd}), \tag{8}$$

where $E_p$ and $E_d$ are the orbital energies of the unperturbed *p* and *d* states, respectively, $c$ is an adjusting factor. In order to apply the model to ternary compound $Zn_{1-x}Cd_xO$, we define an effective *d* states energy and an effective width of upper valence band,

$$E'_d = (E_{3d(\mathrm{Zn})} + E_{4d(\mathrm{Cd})})/2, \tag{9}$$

$$\Delta E' = x\Delta E_{\mathrm{Cd}} + (1-x)\Delta E_{\mathrm{Zn}}, \tag{10}$$

where $E_{3d(\mathrm{Zn})}$ and $E_{4d(\mathrm{Cd})}$ are the orbital energies of the unperturbed *d* states for Zn and Cd, respectively, $x$ is the fraction of Cd in $Zn_{1-x}Cd_xO$; $\Delta E_{\mathrm{Cd}}$ and $\Delta E_{\mathrm{Zn}}$ are the widths of the upper valence bands of CdO and ZnO, respectively, which can be obtained directly from the calculated band structures. In this paper, $E_{2p(\mathrm{O})} = -8.85$ eV, $E_{3d(\mathrm{Zn})} = -10.35$ eV and $E_{4d(\mathrm{Cd})} = -12.33$ eV can be calculated using dmol$^3$ software.[26] Solving Eqs.(6)–(10) simultaneously, we can obtain $q$, $\Delta E_{pd}$ and $V_{pd}$ for different Cd contents. The major error in this approach comes from orbital energies, which can be estimated by different methods. The nonrelativistic Hartree–Fock and Herman–Skillman[27] show that Zn 3*d*/Cd 4*d* have very deep orbital energies, −21.28 eV/−20.76 eV and −17.11 eV/−18.28 eV, respectively. The value obtained from the semirelativistic local density function[25] is −10.48 eV/−11.96 eV, which is close to our calculation. The coefficient $c$ in Eqs.(8) is used to adjust error of orbital energies. The calculated results are listed in Table 3.

**Table 3.** $\Delta E_{pd}$, $V_{pd}$ and $q$ for $Zn_{1-x}Cd_xO$. $\Delta E_{pd}$ is *p-d* repulsion energy, $V_{pd}$ is *p-d* coupling matrix element, and $q$ is the percent of *d* states in the antibonding state. Parameter $c = 1.715$. Results are given in eV.

| | Cd content | | | | | | |
|---|---|---|---|---|---|---|---|
| | 0 | 0.125 | 0.250 | 0.375 | 0.500 | 0.625 | 0.750 |
| $\Delta E_{pd}$ | 0.476 | 0.519 | 0.562 | 0.604 | 0.647 | 0.690 | 0.732 |
| $V_{pd}$ | 2.677 | 2.757 | 2.837 | 2.917 | 2.996 | 3.075 | 3.154 |
| $q$ | 0.031 | 0.034 | 0.038 | 0.041 | 0.045 | 0.048 | 0.051 |

In this paper, the present model is used to analyze the variation of band gap of $Zn_{1-x}Cd_xO$. The top of valence band and *p-d* repulsion energy are fitted by linear equation, as shown in Fig.7. The slope of *p-d* repulsion energy calculated from the fitting equation is equal to that of the top of valance band (see Fig.7), indicating that *p-d* repulsion energy may be used to analyze the shift of the top of the valence band. Previous researches also showed that the *p-d* repulsion in II–VI semiconductors could not be neglected.

Chang *et al*[28] found that the calculated band gap of CdS decreases by 1.2 eV when the $d$ states of Cd are included in the calculation. In $Zn_{1-x}Cd_xO$, valence states through admixture with anti-bonding character into the upper valence band will lead to a destabilization of the crystal, which is in good agreement with the cohesive energy results. In addition, the repulsion between the $\Gamma_{1c}$ and $\Gamma_{1v}$ states has an effect on the variation of the bottom of conduction band,[29] which is lack of systematic analysis now due to complicated interactions of electrons.

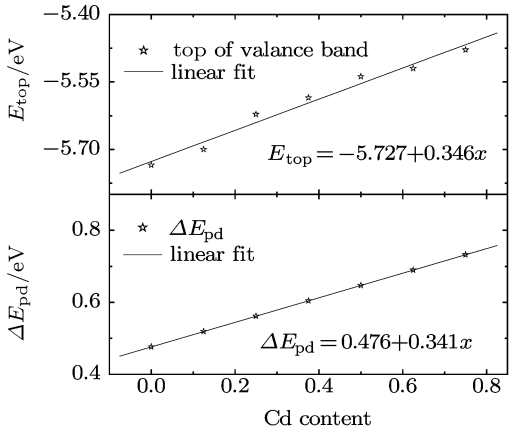



**Fig.7.** The $p$-$d$ repulsion energy and the top of valence band versus Cd content. Solid line is the fitting curve.

## 3.4. Electron density difference

Figure 8 shows electron density difference in $Zn_{1-x}Cd_xO$. It can be found that there is a covalent characteristic in Zn–O bonds and Cd–O bonds. We can also find that the covalent characteristic between Zn–O bonds is more obvious than Cd–O bonds (see Fig.8(h)), which indicates that the cohesive energy of $Zn_{1-x}Cd_xO$ alloys will increase with increasing Cd content. The electron clouds near the Zn, Cd and O atoms show the orientation-dependent characteristic of covalent bond. For $a/b$-axis strain, the bond length between Zn and O in (001) plane will be shortened when $a/b$-axis strain changes in the range from 0.2 to –0.2 (see Figs.8(a)–8(c)). The interaction between Zn and O will be strengthened as $a/b$-axis strain changes from 0.2 to –0.2. For the $c$-axis strain, the electron density difference in (110) plane is shown in Figs.8(e)–8(g). We can find that the electron clouds of O and Zn atoms in (001) plane are different from those in (110) plane, which results in the anisotropy of variation of band gap for ZnO (see Fig.6). It is found by comparing Fig.8(f) with Fig.8(h) that the electronic clouds of O next Cd are compressed, which indicates that $p$-$d$ repulsion for $Zn_{1-x}Cd_xO$ will be strengthened with increasing Cd content. The results is consistent with calculated results (see Table 2).

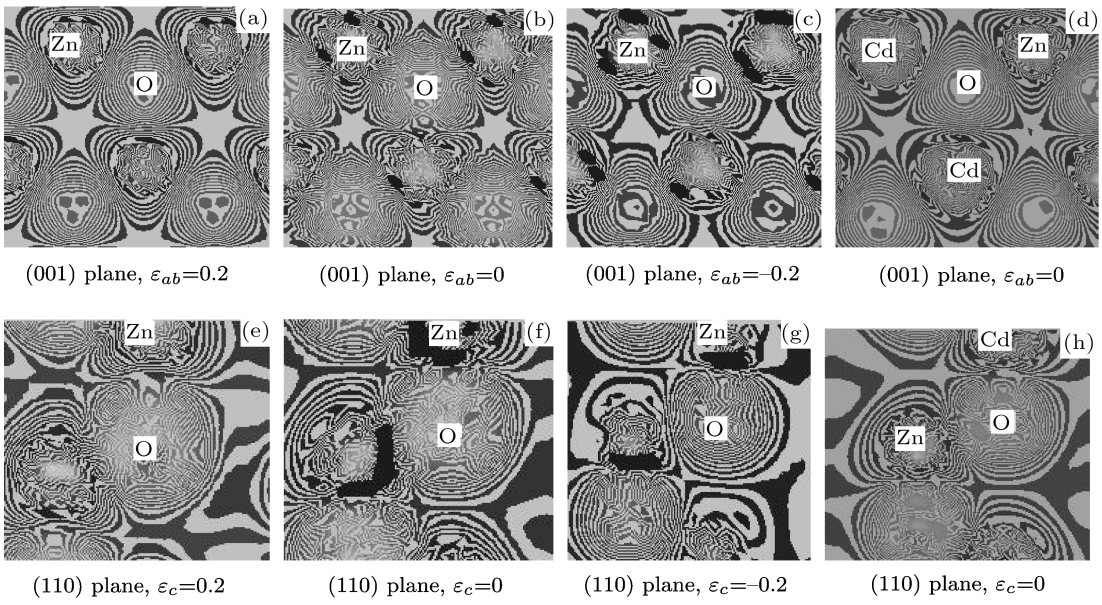



**Fig.8.** Electron density difference for $Zn_{1-x}Cd_xO$. Figures (a), (b), (c) show the electron density difference due to $a/b$-axis strained ZnO in (001) plane; (e), (f), (g) the electron density difference due to $c$-axis strained ZnO in (110) plane; (d) the electron density difference of $Zn_{0.5}Cd_{0.5}O$ in (001) plane; (h) the electron density difference of $Zn_{0.5}Cd_{0.5}O$ in (110) plane.

# 4. Summary

In the present paper, cohesive energy, density of states and band structures of $Zn_{1-x}Cd_xO$ are investigated by CASTEP program based on density functional theory and plane-wave pseudopotential method. The results obtained show that the cohesive energy will rise and the band gap changes from 0.968 eV to 0.043 eV when Cd content changes from 0 to 0.75. The change of band gap is mainly due to lattice tensile strain. In addition, *p*-*d* repulsion model is applied to ternary compound $Zn_{1-x}Cd_xO$. The results show that variation of the top of valance band for $Zn_{1-x}Cd_xO$ can be described by *p*-*d* repulsion energy. Some results can be verified by electron density difference.

# References


[1] Shu J, Wang H T, He J and Tian Y 2005 *Phys. Rev.* B **71** 125132

[2] Ng H T, Han J, Yamada T, Nguyen P, Chen Y P and Meyyappan M 2004 *Nano Lett.* **4** 1247

[3] Wang X D, Summers C J and Wang Z L 2004 *Nano Lett.* **4** 423

[4] Liu C H, B. Liu C, and Fu Z X 2008 *Chin. Phys.* B **17** 2292

[5] Vaithianathan V, Lee B T, Chang C H, Asokan K and Kim S S 2006 *Appl. Phys. Lett.* **88** 112103

[6] Kang H S, Kim G H, Kim D L, Chang H W, Ahn B D and Lee S Y 2006 *Appl. Phys. Lett.* **89** 181103

[7] Xiao Z Y, Liu Y C, Mu R, Zhao D X and Zhang J Y 2008 *Appl. Phys. Lett.* **92** 052106

[8] Zúñiga-Péreza J, Muñoz-Sanjosé V, Lorenz M, Benndorf G, Heitsch S, Spemann D and Grundmann M 2006 *J. Appl. Phys.* **99** 023514

[9] Sadofev S, Schäfer P, Fan Y H, Blumstengel S and Henneberger F 2007 *Appl. Phys. Lett.* **91** 201923

[10] Ma D W, Ye Z Z, Huang J Y, Zhao B H, Wan S K, Sun X H and Wang Z G 2003 *Chin. Phys. Lett.* **20** 942

[11] Zhu Y Z, Chen G D and Ye H 2008 *Phys. Rev.* B **77** 245209

[12] Zhang X D, Guo M L, Li W X and Liu C L 2008 *J. Appl. Phys.* **103** 063721

[13] Perdew J P, Burke K and Ernzerhof M 1996 *Phys. Rev. Lett.* **77** 3865

[14] Ji Z H, Zeng X H, Hu Y J and Tan M Q 2008 *Acta Phys. Sin.* **57** 3753 (in Chinese)

[15] Payne M C, Teter M P, Allan D C, Arias T A and Joannopoulos J D 1992 *Rev. Mod. Phys.* **64** 1045

[16] Schulz H and Thiemann K H 1979 *Solid State Commun.* **32** 783

[17] Schleife A, Fuchs F, Furthmüller J and Bechstedt F 2006 *Phys. Rev.* B **73** 245212

[18] Padam D K, Malhotra G L and Rao S U M 1988 *J. Appl. Phys.* **63** 770

[19] Duan M Y, Xu M, Zhou H P and Shen Y B 2007 *Acta Phys. Sin.* **56** 5359 (in Chinese)

[20] Ohomo A, Kawasaki M, Koida T, Masubuchi K, Koinuma H, Sakurai Y and Segaw Y 1998 *Appl. Phys. Lett.* **72** 2466

[21] Ma D W, Ye Z Z and Chen L L 2004 *Phys. Status Solidi* A 201 2929

[22] Liu X J, Song C, Zeng F, Pan F, He B and Yan W S 2008 *J. Appl. Phys.* **103** 093911

[23] Li Y F, Yao B, Lu Y M, Cong C X, Zhang Z Z, Gai Y Q, Zheng C J, Li B H, Wei Z P, Shen D Z and Fan X W 2007 *Appl. Phys. Lett.* **91** 021915

[24] Dalpian G M, Yan Y and Wei S H 2006 *Appl. Phys. Lett.* **89** 011907

[25] Wei S H and Zunger A 1988 *Phys. Rev.* B **37** 8958

[26] Delley B J 2000 *J. Chem. Phys.* **113** 7756

[27] Hedin L and Lundqvist B I 1971 *J. Phys.* C **4** 2063

[28] Chang K J, Froyen S and Cohen M L 1983 *Phys. Rev.* B **28** 4736

[29] Yan Y, Dalpian G M, Jassim M M A and Wei S H 2004 *Phys. Rev.* B **70** 193206